ARMY RESEARCH LABORATORY

The Effect of Turbulent Intermittency on Detection in Acoustic Shadows

by D. Keith Wilson
Battlefield Environment Directorate

ARL-TR-1002 May 1996

NOTICES

Disclaimers

The findings in this report are not to be construed as an official Department of the Army position, unless so designated by other authorized documents.

The citation of trade names and names of manufacturers in this report is not to be construed as official Government indorsement or approval of commercial products or services referenced herein.

Destruction Notice

When this document is no longer needed, destroy it by any method that will prevent disclosure of its contents or reconstruction of the document.

REPORT DOCUMENTATION PAGE

Form Approved
OMB No. 0704-0188

1. AGENCY USE ONLY (Leave blank)	2. REPORT DATE	3. REPORT TYPE AND DATES COVERED
	May 1996	Final

4. TITLE AND SUBTITLE

The Effect of Turbulent Intermittency on Detection in Acoustic Shadows

5. FUNDING NUMBERS

6. AUTHOR(S)

D. Keith Wilson

7. PERFORMING ORGANIZATION NAME(S) AND ADDRESS(ES)

U.S. Army Research Laboratory
Battlefield Environment Directorate
Attn: AMSRL-BE-S
White Sands Missile Range, NM 88001-5501

8. PERFORMING ORGANIZATION REPORT NUMBER

ARL-TR-1002

9. SPONSORING / MONITORING AGENCY NAME(S) AND ADDRESS(ES)

U.S. Army Research Laboratory
2800 Powder Mill Road
Adelphi, MD 20783-1145

10. SPONSORING / MONITORING AGENCY REPORT NUMBER

ARL-TR-1002

11. SUPPLEMENTARY NOTES

12a. DISTRIBUTION / AVAILABILITY STATEMENT

Approved for public release; distribution unlimited.

12b. DISTRIBUTION CODE

A

13. ABSTRACT *(Maximum 200 words)*

This report discusses the effect of turbulent intermittency (the tendency of turbulence to occur in bursts of activity) on large-angle acoustic scattering and source detection and shows how intermittency increases the occurrence of high–intensity scattering events. Source detection probabilities strongly depend on the occurrence of these events, as well as the noise background characteristics. Detection probability calculations are made for a variety of noise scenarios. Intermittency increases the detection probabilities by several orders of magnitude if the signal-to-noise ratio (SNR) is low and the noise background has relatively little variance. The intermittency effect becomes less significant in high SNR situations and highly variable noise environments. This report also discusses estimation of the parameters required by the intermittency theory from standard micrometeorological measurements.

14. SUBJECT TERMS

acoustic, detection, shadow zone, turbulence, intermittency, scattering

15. NUMBER OF PAGES

48

16. PRICE CODE

17. SECURITY CLASSIFICATION OF REPORT	18. SECURITY CLASSIFICATION OF THIS PAGE	19. SECURITY CLASSIFICATION OF ABSTRACT	20. LIMITATION OF ABSTRACT
Unclassified	Unclassified	Unclassified	SAR

Acknowledgments

The author is indebted to J. C. Wyngaard of Penn State for explaining the fundamentals of turbulent intermittency. D. I. Havelock of National Research Council Canada provided the experimental data.

Contents

Figures

Table

1. Introduction

Most descriptions of wave propagation through turbulence are based on a nonintermittent description of the turbulence. Intermittency refers to the tendency of turbulence to occur in bursts of activity, surrounded by relatively quiet regions. The effect of intermittency on wave propagation is to create regions in space and time where there is particularly strong scattering and spreading of the propagating wave. In this manner, intermittency can strongly affect probabilities of detection of enemy assets (by acoustic and optic methods), the performance of targeting systems, and radio communications.

Figures 1 and 2 illustrate the conceptual difference between the nonintermittent and intermittent descriptions of scattering. The figures show scattering of helicopter noise, with the receiver hidden from the helicopter by an intervening hill. In the nonintermittent description, the eddies responsible for the scattering are smoothly distributed throughout space. In the more realistic intermittent description, the eddies occur in bunches. If a high concentration of eddies is located within the scattering volume (as determined by the source/receiver geometry, beam patterns, and topography), scattering will be enhanced. On the other hand, a low concentration of eddies results in reduced scattering. As the turbulent field evolves, regions of high and low eddy concentration move in and out of the scattering volume.

A preliminary study by Wilson, Wyngaard, and Havelock (1995) of acoustic scattering into a ground-based shadow zone showed that intermittency can increase the fourth moment of the scattered intensity (a measure of the frequency of occurrence of high-scattered-intensity events) 100 fold. Why, if intermittency has such a profound affect on scattering statistics, has it largely been neglected until now? There are several reasons:

- Scattering by intermittent turbulence is a difficult cross-disciplinary problem, involving forefront research in turbulence and wave scattering. Most of the outstanding, original work in scattering by turbulence was completed two to three decades ago, by scientists who studied turbulence theory before the role of intermittency became widely recognized.

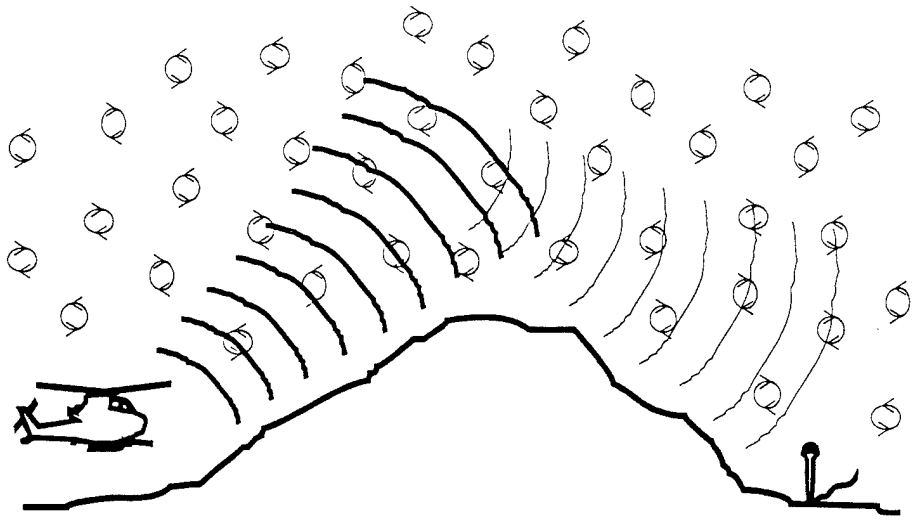

Figure 1. Scattering by nonintermittent turbulence. A helicopter generates noise that is scattered by eddies and received by a microphone on the other side of a hill. The eddies are smoothly distributed through space.

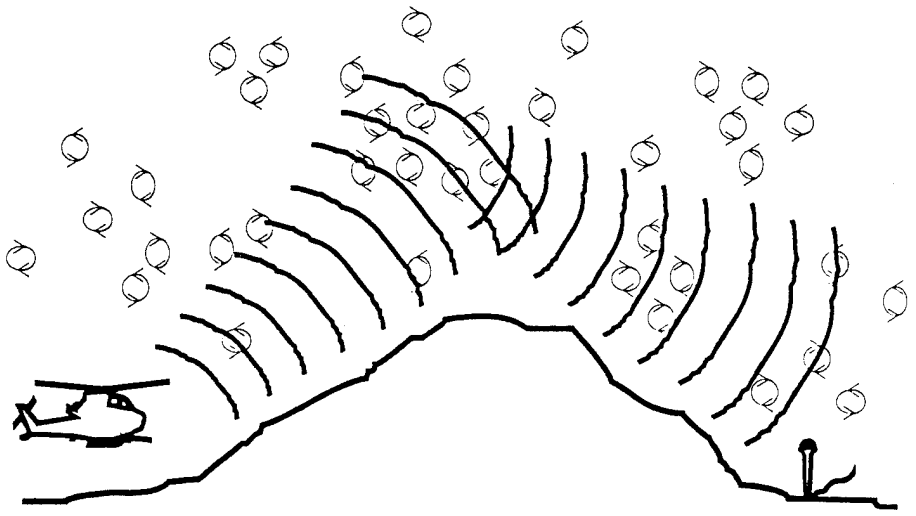

Figure 2. Scattering by intermittent turbulence. The eddies occur in bunches. If a high concentration of eddies occurs at the intersection of the source and receiver beams, scattering is enhanced.

- The theory of intermittent turbulence was developed largely by Soviet scientists such as Kolmogorov (1962), Obukhov (1962), and Gurvich and Yaglom (1967), and their work has been slow to percolate into the mainstream English literature.

- Intermittency becomes most important when the scattering volume has dimensions comparable to or smaller than the largest scales of the turbulent flow. This is not the case for many radio wave scattering problems considered in the past; however, it is quite frequently the case in atmospheric acoustics, which has not been so deeply studied. It is now becoming a more significant issue in radar design and data interpretation, as the resolution of these systems improves.

This report considers the effect of turbulent intermittency on acoustic wave scattering. The case considered is a particularly simple, but practically important, one: that of a source hidden from a receiver by virtue of an acoustic shadow. *Shadow* has the same meaning here as in the optical case: no direct beam traveling from the source to the receiver. Acoustic shadows are normally formed as a result of topography, such as hills, or as a result of upward refraction of sound waves. Upward refraction results when sound propagates upwind or the temperature decreases with height. It recently has been well established that most of the sound energy reaching a receiver in an acoustic shadow is scattered there by turbulence (Gilbert, Raspet, and Di 1990).

This report begins in section 2, with a brief, qualitative description of turbulent intermittency and its effect on scattering statistics. (Refer to Wilson and Thomson (1995) for a more rigorous and theoretical discussion.) Section 3, considers the effect of intermittency on source detection probabilities, the main topic of this report. Lastly, section 4 discusses the methods for estimating the parameters required by the intermittency theory.

2. Effect of Intermittency on Scattering Statistics

The intensity of the signal at a receiver fluctuates randomly as a result of scattering by turbulence, regardless of the presence of significant intermittency. In nonintermittent scattering, the scattered acoustic pressure has simple, normal statistics.* This implies that the scattered intensity (proportional to the pressure magnitude squared) has an exponential probability distribution function (pdf) (Tatarskii 1971):

$$P(I) = \frac{1}{I_0}\exp\left(-\frac{I}{I_0}\right) \tag{1}$$

where

I = the intensity at the receiver

$I_0 = \langle I \rangle$ = the ensemble mean.

The mean scattered intensity is proportional to the sum of the structure-function parameters for temperature, C_T^2, and for velocity, C_V^2:†

$$I_0 = \langle I \rangle = P\left(a_T C_T^2 + a_V C_V^2\right) \tag{2}$$

where

Π = the source power

The a's depend on the source wavelength and scattering angle (Ostashev 1994).

In nonintermittent treatments, the structure-function parameters are defined as ensemble-mean quantities. Intermittency enters into the problem when the structure-function parameters vary in space and time. The time and space

* Normal pressure statistics occur when the scattering is saturated. In that case the standard deviation of the received intensity fluctuations, divided by the mean intensity, is unity, and does not change significantly as one moves further away from the source. The pressure signal is generally saturated whenever the receiver is in an acoustic shadow, and the dominant contribution to the signal is turbulent scattering.

† The structure function parameter for temperature is defined by the equation

$$\left\langle \left(T(r) - T(0)\right)^2 \right\rangle = C_T^2 r^{2/3}$$

where the separation r must be small compared to the integral length scale of the turbulence. A similar equation is used to define C_V^2, with the added stipulation that the spatial separation is in the same direction as the velocity component.

variability is how we quantify such loosely defined quantities as the "eddy concentration" discussed in connection with figures 1 and 2. From the intermittent standpoint, equation (2) is rewritten

$$\tilde{I}_0 = \left\langle I \middle| \tilde{C}_T^2, \tilde{C}_V^2 \right\rangle = \Pi\left(a_T \tilde{C}_T^2 + a_v \tilde{C}_V^2\right). \tag{3}$$

In the above, locally varying quantities are distinguished from their ensemble means using tildes. The meaning of the vertical bar is that the variable on the left is conditionally sampled with respect to the variables on the right. Each time specific values $(\tilde{C}_T^2, \tilde{C}_V^2)$ occur, we record I. The ensemble mean of these conditionally sampled values of I is designated $\tilde{I}_0$, the local mean intensity. Like the local structure function parameters, the local mean intensity varies in space and time. Because the exponential probability law holds for fixed values of the structure function parameters, it follows immediately from equation (1) that

$$P(I|\tilde{I}_0) = P(I|\tilde{C}_T^2, \tilde{C}_V^2) = \frac{1}{\tilde{I}_0} \exp\left(-\frac{I}{\tilde{I}_0}\right). \tag{4}$$

However, we would also like to know the unconditioned pdf for the intensity, *P(I)*. This follows from the statistical identity

$$P(I) = \int_0^\infty P(I|\tilde{I}_0) P(\tilde{I}_0) d\tilde{I}_0 . \tag{5}$$

To proceed, we need to know $P(\tilde{I}_0)$, which, by equation (3), requires models for $P\left(\tilde{C}_T^2\right)$ and $P\left(\tilde{C}_V^2\right)$.

Kolmogorov (1962) originally suggested that the local structure function parameters followed a log-normal distribution. In recent years, certain shortcomings in the log-normal model have become evident, and alternatives have been proposed (Romano 1995). The log-normal model will be used in this report; however, for simplicity, the newer models are fairly complex, not as well tested, and affect mainly statistics of very high order.

Having decided on the log-normal model for the structure function parameters, there is still a further complication in determining $P(\tilde{I}_0)$. Specifically, it is not generally the case that the sum of two log-normal variables is log-normal.* Wilson (1995) considered the pdf of $\tilde{I}_0$ in detail, however, and found that for reasonable values of a_T or a_V, it was log-normal to a very acceptable degree of approximation. We therefore assume $P(\tilde{I}_0)$ is also log-normal:

$$P(\tilde{I}_0) = \frac{1}{\sqrt{2\pi}\sigma\tilde{I}_0} \exp\left[-\frac{\left(\log \tilde{I}_0 - \left\langle \log \tilde{I}_0 \right\rangle\right)^2}{2\sigma^2} \right] \qquad (6)$$

where

σ^2 = the variance of $\log \tilde{I}_0$.

The parameter σ characterizes the strength of the intermittency. It can be shown that $\log\langle I\rangle = \left\langle \log \tilde{I}_0 \right\rangle + \sigma^2/2$ for the log-normal distribution (Wilson, Wyngaard, and Havelock 1995). If $\langle I\rangle$ = const, this relationship allows us to compute the value for $\left\langle \log \tilde{I}_0 \right\rangle$ needed in equation (6) as a function of σ.

One drawback of the log-normal distribution is that it is not possible to perform the integration in equation (5) analytically. Fortunately, it is not particularly difficult to perform a numerical integration in this case. Equation (5) was analytically converted to an integration over $u = \log \tilde{I}_0$, and a simple, 1000-step trapezoidal integration from $u = \left\langle \log \tilde{I}_0 \right\rangle - 6\sigma$ to $u = \left\langle \log \tilde{I}_0 \right\rangle + 6\sigma$ was applied.

Figure 3 shows $P(I)$ calculated in this manner for various values of the parameter σ. The main effect of intermittency is to enhance the probability of occurrence of very large values of the scattered intensity. To make the effect of intermittency more graphically evident, the ordinate on figure 3 was plotted in logarithmic coordinates. In the logarithmic coordinates, the nonintermittent pdf equation (1) appears as a straight line.

* Unlike normal random variables, the sum of two jointly log-normal random variables is not itself log nomal.

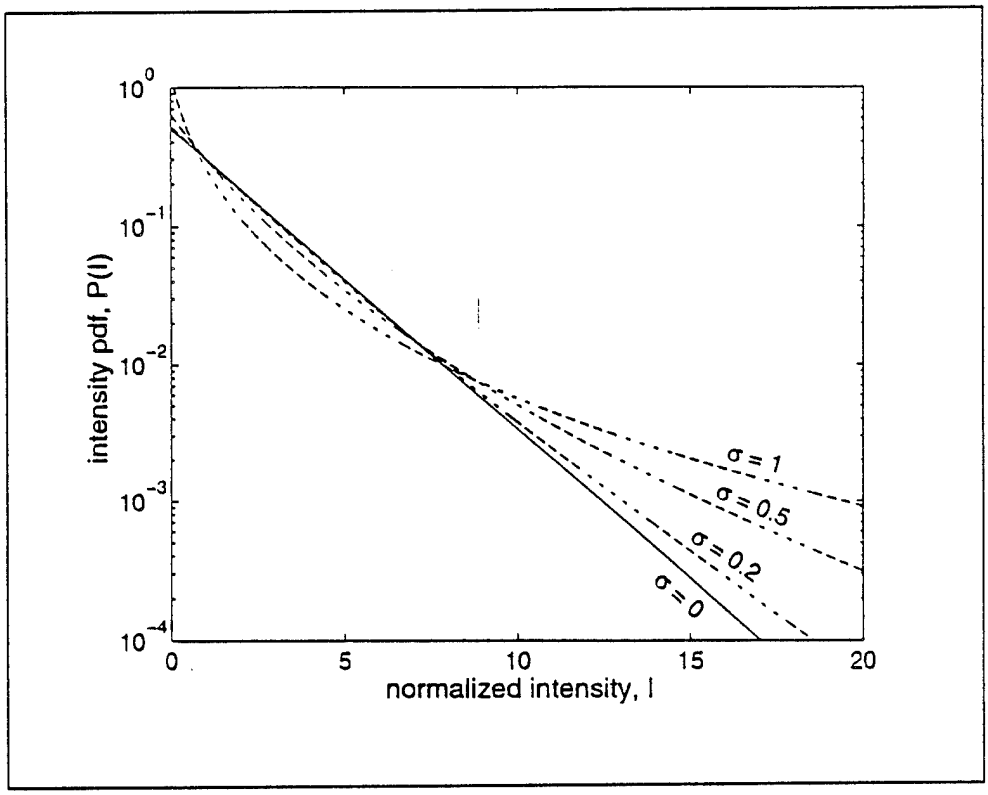

Figure 3. Nonintermittent (solid line) and intermittent (dashed lines) probability density functions of the received intensity. The parameter σ is a measure of the amount of intermittency. Intensity is normalized so its ensemble mean value $\langle I \rangle = 2$.

The calculations for figure 3 were performed so the mean intensity at the receiver $\langle I \rangle$ was the same, regardless of the intermittency parameter σ. We would really like to compare pdf for constant source power P, and constant ensemble mean structure-function parameters C_T^2 and C_V^2. To see the relationship between the two approaches, first consider the ensemble average of equation (3):

$$\left\langle \tilde{I}_0 \right\rangle = \Pi\left(a_T \left\langle \tilde{C}_T^2 \right\rangle + a_V \left\langle \tilde{C}_V^2 \right\rangle \right). \tag{7}$$

By substituting equation (4) into equation (5), and integrating $IP(I)$ over I, it can be shown that $\langle I \rangle = \left\langle \tilde{I}_0 \right\rangle$. Furthermore, by definition $\left\langle \tilde{C}_T^2 \right\rangle = C_T^2$; likewise for C_V^2. Equation (2), which can be derived by taking the ensemble mean of equation (3), still holds, regardless of whether intermittency is present. If the quantities on the right-hand side of equation (2) (the source power and the mean structure-function parameters) are taken as constants, the left-hand side

(the mean received intensity) must also be constant. Hence, it follows that holding the mean intensity at the receiver constant, while varying the intermittency parameter σ, is equivalent to holding the source power and mean structure-function parameters constant, while varying σ.

Figure 4 shows pdfs for the received intensity recorded in an acoustic shadow zone (Wilson, Wyngaard, and Havelock 1995). The results for two separate measurement periods are shown: WI, a low intermittency case; and SI, a high intermittency case. The values of σ used to generate the theoretical predictions were 0.10 and 0.56, respectively. Both datasets show a clear departure from the straight line characteristic of the nonintermittent pdf.

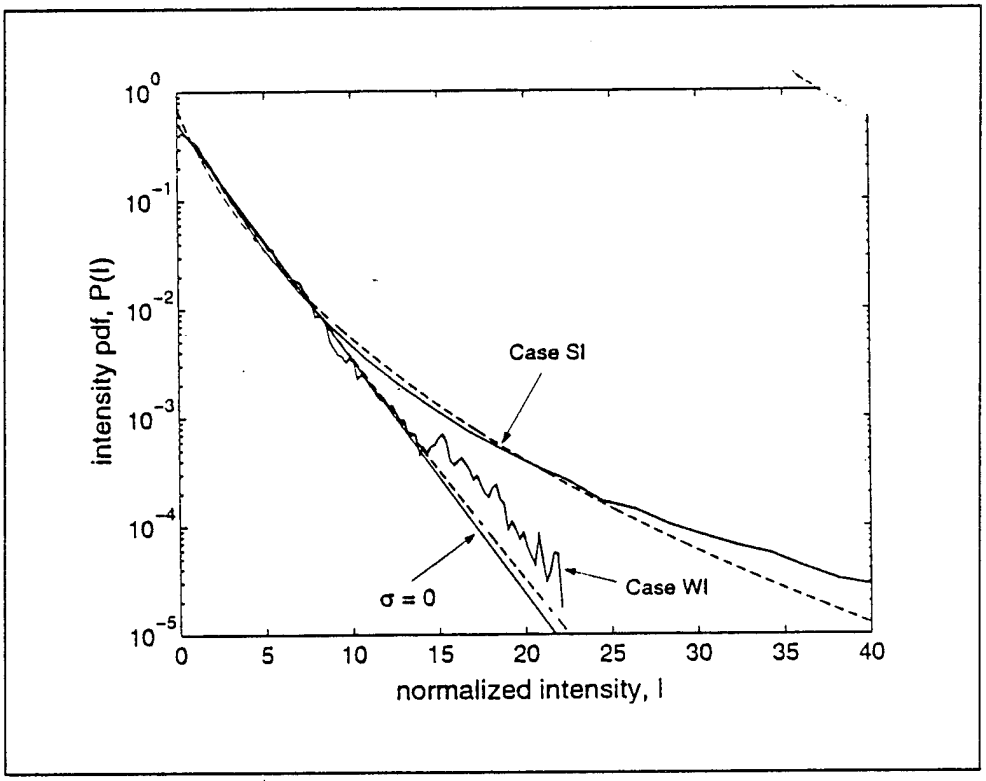

Figure 4. Experimentally determined pdfs for scattered intensity (solid line) and theoretical fits (dashed lines). The straight, solid line is the nonintermittent prediction. Intensity is normalized so its ensemble mean value $\langle I \rangle = 2$.

Section 4 discusses how the parameter σ varies in response to the scattering geometry and meteorological conditions. Intermittency was probably more significant in the SI case because it was recorded later in the morning than WI,

when the atmospheric boundary layer was thicker and larger eddies were present. The large eddies drive the intermittency.

3. Source Detection Probabilities

In this section, the effect of turbulent intermittency on detection of scattered signals in a noisy environment is discussed. The first case considered is a constant noise background. Although rather unrealistic, the constant noise background case serves to illustrate the basic procedure of computing detection probabilities and the role of intermittency. The second case considered is noise having a Nakagami (1960)/Rice (1945) distribution, which can be used for a variety of noise scenarios by varying its parameters. The computation for the Nakagami/Rice distribution is considerably more complicated, but probably more realistic for battlefield conditions.

One important simplifying assumption in the following calculations is that the source will be detected when its intensity (loudness) in some frequency band exceeds the noise in that same band. This neglects gains that can be achieved in system design and signal processing (e.g. beam forming, matched filtering). Furthermore, this may also restrict the calculations to narrow-band detection schemes. The probabilities for detection of broad-band signals would be the same only if the scattering strength for all of the frequency components increases and decreases simultaneously. In other words, there must be coherency across the band of frequencies used in the detection scheme; otherwise, the calculation of detection probabilities depends heavily on the signal processing algorithm and the cross-frequency coherence. Presently, the characteristics and quantification of cross-frequency coherence for scattering by atmospheric turbulence are rather poorly understood and will be an important topic for future research.

Given the simplifying assumptions, the general problem can be formulated as follows. Let $P(I,I_N)$ be the joint pdf for the scattered intensity, I, and the noise intensity background, I_N. The detection probability is

$$P(I > I_N) = \int_0^\infty \int_0^\infty P(I, I_N)\, H(I - I_N)\, dI\, dI_N \qquad (8)$$

where

$H(I-I_N)$ = the Heaviside function (1 if $I > I_N$, and zero otherwise).

Assuming the scattering and noise are independent processes, $P(I,I_N) = P(I)P(I_N)$. The integral then can be rewritten as

$$P(I > I_N) = \int_0^\infty P(I > I_N | I)\, P(I)\, dI \tag{9}$$

in which the probability of the scattered intensity exceeding the noise intensity, conditioned to a fixed value of the scattered intensity, is

$$P(I > I_N | I) = \int_0^I P(I_N)\ dI_N\ . \tag{10}$$

3.1 Constant Noise Background

Suppose the intensity of the noise level at the receiver, in the same frequency band as the source, is constant and equal to $\langle I_N \rangle$. For this case, $P(I_N) = \delta\left(I_N - \langle I_N \rangle\right)$. The integral in equation (10) then evaluates to 1 if $I > \langle I_N \rangle$; otherwise, it is zero. The probability of detecting the source, given by equation (9), is as follows:

$$P(I > I_N) = \int_{\langle I_N \rangle}^\infty P(I)\, dI\,. \tag{11}$$

This integration can be performed easily for the nonintermittent case. Using the exponential pdf for I, equation (1), the result is $P(I > I_N) = \exp\left(-\langle I_N \rangle / I_0\right)$. For the intermittent case, substitute for $P(I)$ using equation (5), switch the order of integration between I and $\tilde{I}_0$, and perform the integration over I explicitly. Equation (12) becomes the following integral over $\tilde{I}_0$:

$$P(I > I_N) = \int_0^\infty \exp\left(-\frac{\langle I_N \rangle}{\tilde{I}_0}\right) P(\tilde{I}_0)\, d\tilde{I}_0\ . \tag{12}$$

For the log-normal distribution equation (6), the integration must be done numerically. Figure 5 shows the results of the integration for a few different values of σ. The abscissa on the plot is the mean signal-to-noise ratio (SNR), $\langle I \rangle / \langle I_N \rangle$.

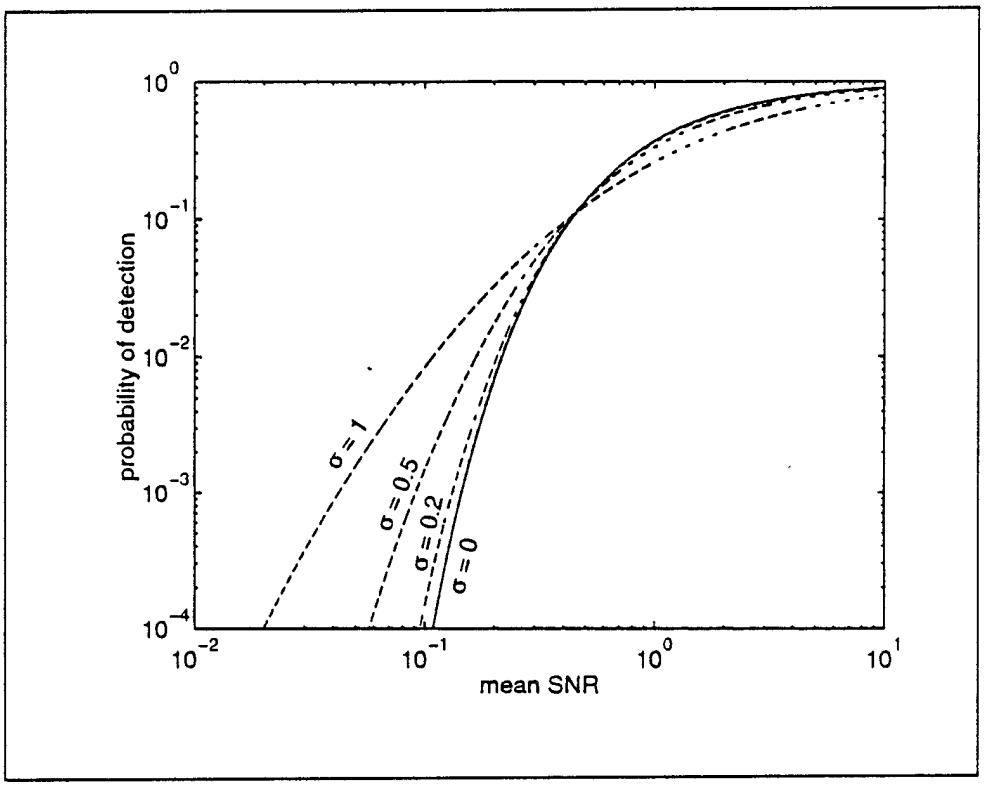

Figure 5. Nonintermittent (solid line) and intermittent (dashed lines) probabilities of detection as a function of the mean SNR, for the constant noise model. Intensity is normalized so its ensemble mean value is 2.

Figure 5 demonstrates the profound effect intermittency has on probabilities of detection, particularly at low SNRs. For an SNR = 0.1, the probability of detection at high values of intermittency ($\sigma = 1$) is more than 100 times greater than the probability with no intermittency. Even at moderate values of intermittency ($\sigma = 0.5$), the detection probability is enhanced more than 20 fold.

The detection probabilities shown in figure 5 apply to a single, statistically independent sample. Perhaps a better idea of the significance of the intermittency effect can be obtained if the number of statistically independent samples M required to achieve a specified detection probability P_D is considered. It can be shown that

$$P_D = 1 - \left[1 - P(I > I_N)\right]^M \tag{13}$$

and therefore

$$M = \frac{\log(1 - P_D)}{\log[1 - P(I > I_N)]}. \qquad (14)$$

Figure 6 shows the minimum values of M required to obtain a probability of detection of $P_D = 0.9$. The figure demonstrates, for example, that approximately five times as many samples need to be collected at a mean SNR = 0.1 if there is no intermittency, as compared to when there is strong intermittency ($\sigma = 1$). When the SNR is more favorable, the situation actually reverses. Approximately 60 percent more samples are needed when $\sigma = 1$ as compared to $\sigma = 0$.

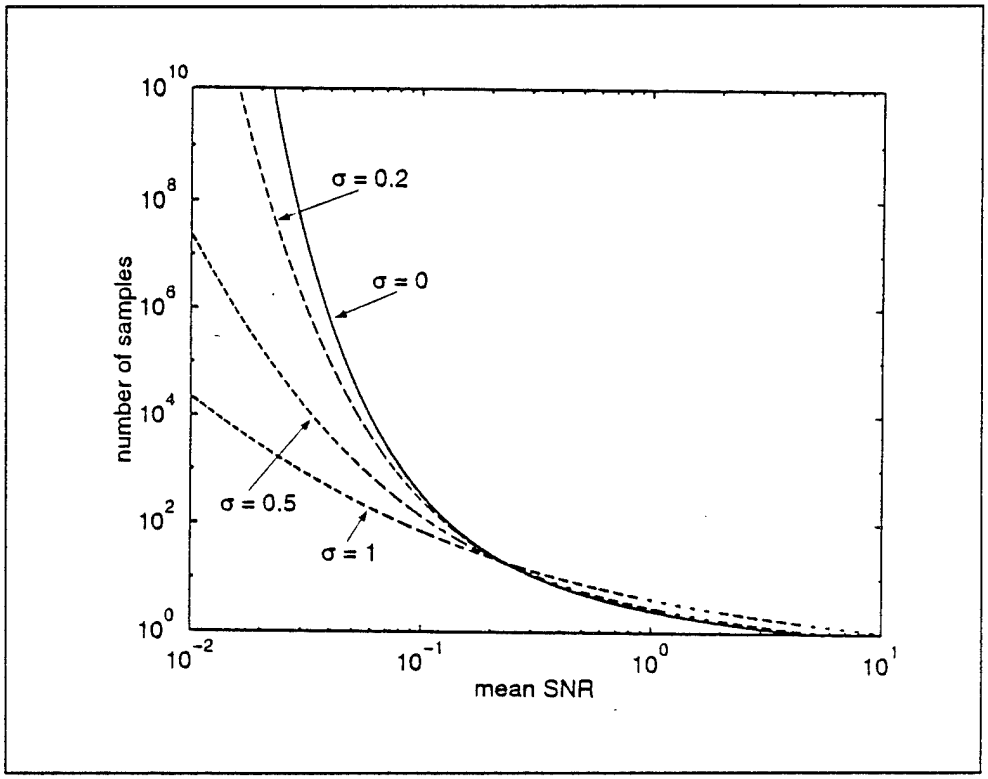

Figure 6. Number of statistically independent samples required to achieve a 90 percent probability of detection, as a function of the mean SNR.

In practice, data are normally collected over a time interval rather than as isolated, statistically independent samples. M can be converted to a time collection interval T using the following formula:

$$T = M\tau \qquad (15)$$

where

τ = the integral time scale associated with the fluctuations in intensity.

We may estimate the time scale for scattering by inertial subrange turbulence using the following formula (Wilson, Wyngaard, and Havelock 1995):

$$\tau = \left(\frac{\lambda^2}{4\varepsilon}\right)^{1/3} \tag{16}$$

where

λ = the acoustic wavelength

ε = the dissipation rate of turbulent kinetic energy (discussed in the section 3.2).

For a frequency of 500 Hz, $\lambda \approx 2/3$ m. Taking $\varepsilon = 10^{-3}$ m^2/s^3 as a representative value, $\tau = 5$ s. The curves in figure 6 show that approximately 1750 s are required for a 90 percent detection probability in the nonintermittent case with SNR = 0.1, whereas only 350 s would be required in the highly intermittent case.

3.2 Variable Noise Background

The constant noise model considered in section 3.1 is unrealistic for most battlefield environments. In actuality, there will be time-varying noise at the receiver caused by assets, friendly or foe, and by turbulent pressure fluctuations. Hence, in this subsection, the effect of noise variance on the detection calculations is considered.

The Nakagami (1960)/Rice (1945) distribution, which corresponds to a fixed mean amplitude for the noise with normally distributed in-phase and quadrature components, is the variable noise model used. The Nakagami/Rice distribution yields the pdf for the noise intensity

$$P(I_N) = \frac{1}{2\sigma_N^2}\exp\left(-\frac{I_N + M}{2\sigma_N^2}\right) I_0\left(\frac{\sqrt{I_N M}}{\sigma_N^2}\right) \tag{17}$$

where

σ_N^2	=	the variance parameter for the noise
M	=	the mean amplitude parameter squared
$I_0()$	=	the 0-order modified Bessel function of the first kind.

Figure 7 shows example curves for the Nakagami/Rice intensity pdf. When M/σ_N^2 is small, the pdf is essentially an exponential distribution, which should work well in cases where random, loud noise events are superimposed on a relatively quiet background. The large M/σ_N^2 case corresponds to noise events superimposed on a relatively loud background. (The word "relatively" must be stressed here: the balance between the noise events and the background, not their actual levels, is the only important factor for determining the scaled pdf.)

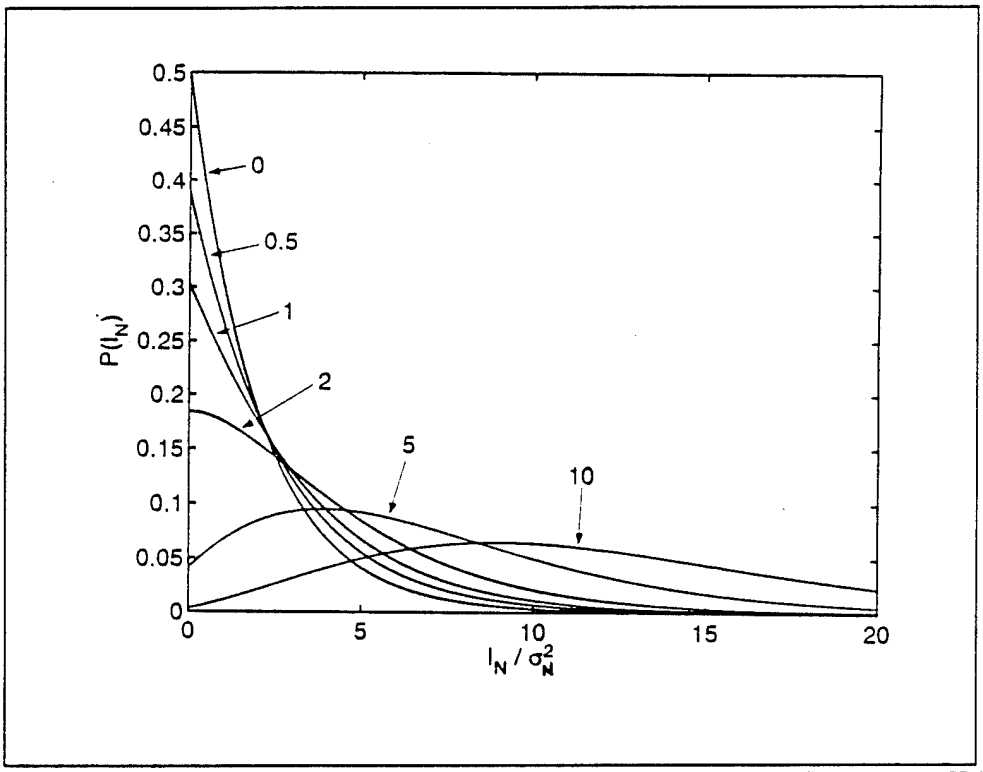

Figure 7. Variable noise model based on the Nakagami/Rice distribution. The curves represent different values of the ratio M/σ_N^2.

Unlike the constant noise case, the integrations over I and I_N cannot be accomplished analytically. We are left with a triple integral that cannot be analytically simplified because we must also integrate over $\tilde{I}_0$ to calculate the

detection probability. It would be computationally prohibitive to solve the triple integral numerically. Alternatively, the problem can be solved using a Monte Carlo method to generate a series of random numbers for $\tilde{I}_0$, I, and I_N which follow the appropriate distributions (log-normal, exponential, and Nakagami/Rice, respectively). Then one counts the fraction of cases where $I > I_N$. I wrote a short (approximately 25 lines) script in Matlab® to accomplish this task.

The detection probability for $M/\sigma_N^2 = 0.5$ is plotted as a function of mean SNR, $\langle I \rangle / \langle I_N \rangle$, in figure 8. The slight "wiggle" in the curves is an artifact of the Monte Carlo technique. The wiggles can be diminished by averaging a larger number of random samples. In this small M/σ_N^2 case, varying the intermittency strength parameter σ^2 has extremely little effect on detection probabilities. In contrast, when $M/\sigma_N^2 = 5$, the case shown in figure 9, intermittency has a pronounced effect. The results for large M/σ_N^2, in fact, converge on the constant noise background case shown in figure 5.

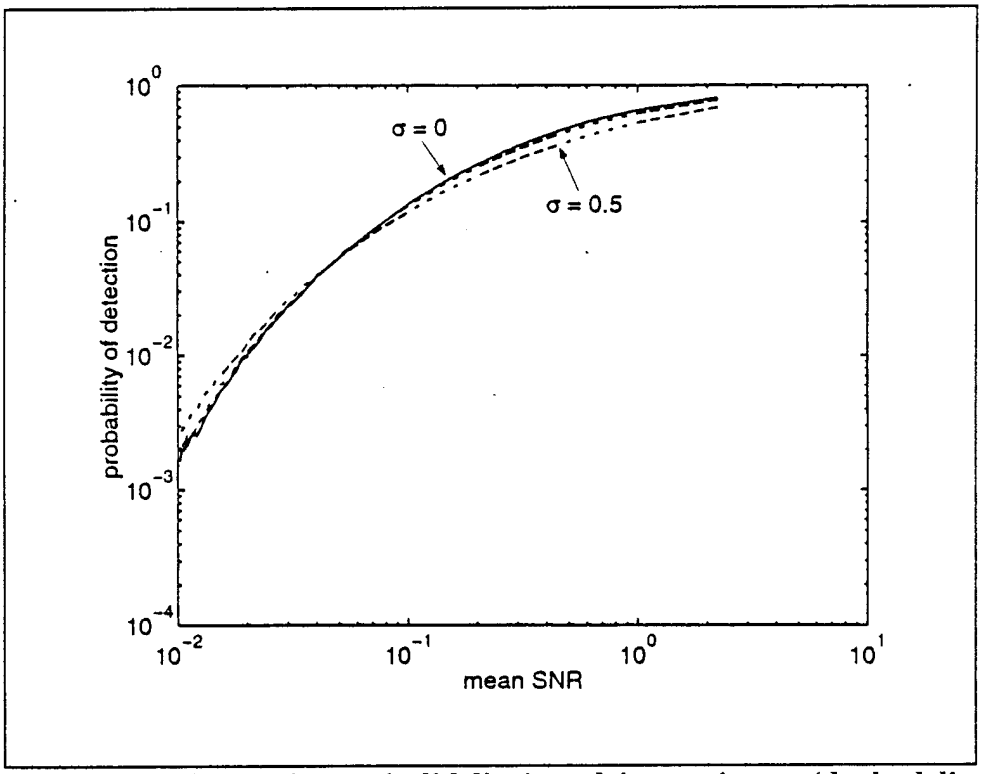

Figure 8. Nonintermittent (solid line) and intermittent (dashed lines) probabilities of detection as a function of the mean SNR, for the variable noise model with $M/\sigma_N^2 = 0.5$.

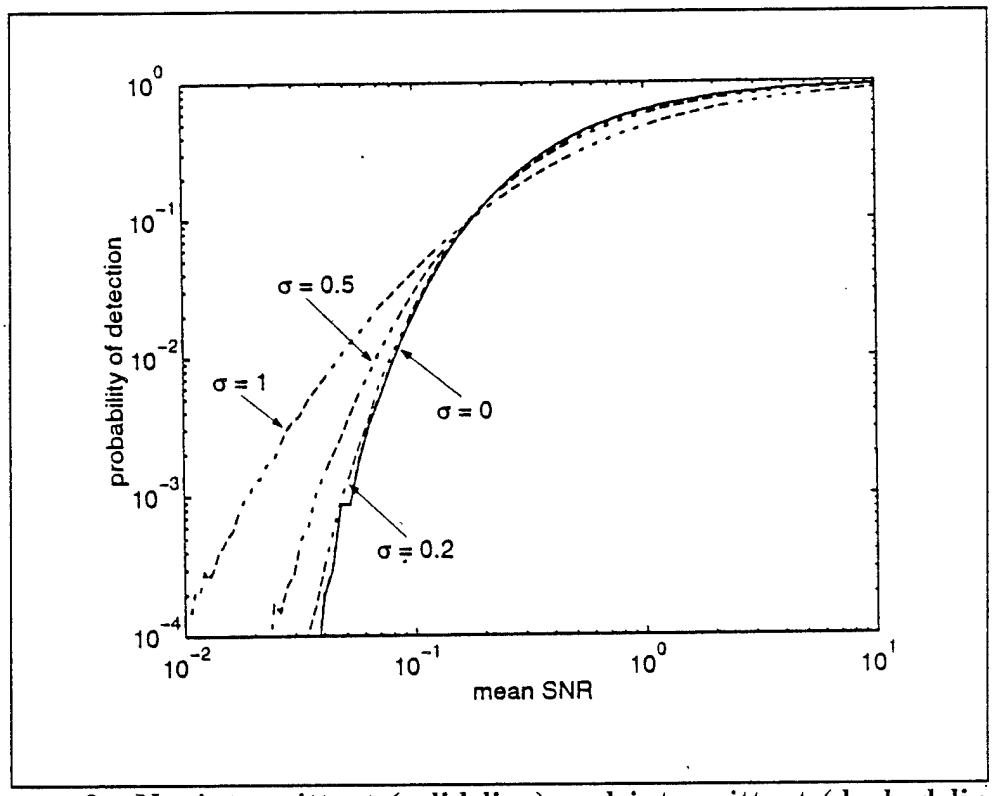

Figure 9. Nonintermittent (solid line) and intermittent (dashed lines) probabilities of detection as a function of the mean SNR, for the variable noise model with $M/\sigma_N^2 = 5$.

Hence, the following conclusion: Intermittency becomes less significant when the variance in the noise exceeds the scattered signal variance resulting from intermittency effect. This can be understood intuitively. In environments in which the noise is highly variable, the detection of a source depends mostly on whether there is a competing noise event, rather than on the existence of intermittent episodes of enhanced scattering.

4. Parameter Estimation

In this section, estimation of the parameters required by the intermittency theory is considered. Parameters for noise distributions are omitted from the discussion though. The noise parameters are neglected not because they are thought unimportant, but rather because they are beyond the scope of this report.

As discussed earlier, the log-normal distribution has the property

$$\sigma^2 = 2\left(\log\langle I\rangle - \left\langle \log \tilde{I}_0 \right\rangle\right). \tag{18}$$

Wilson (1995) showed that when intermittency in both the temperature and velocity fields is present,

$$\left\langle \log \tilde{I}_0 \right\rangle \approx \log\left(a_T' + a_v'\right) + \frac{a_T' a_v'}{2\left(a_T' + a_V'\right)^2} \tag{19}$$

where

σ_T^2 = the variance in $\log \tilde{C}_T^2$

σ_V^2 = the variance in $\log \tilde{C}_V^2$

$$a_T' = a_T C_T^2 \exp\left(-\sigma_T^2 / 2\right) \tag{20}$$

and likewise for a_V'.

Estimates for the log-variances of the structure-function parameters are $\sigma_T^2 \approx (7/9)\sigma_s^2$ and $\sigma_V^2 \approx (4/9)\sigma_s^2$, where σ_s^2 is the log-variance of the log rate of dissipation of turbulent kinetic energy (TKE), given by Kolmogorov (1962) as

$$\sigma_s^2 \approx \mu \log(\ell / r) \tag{21}$$

where

$\mu \cong 0.2$ (Anselmet *et al.* 1984)

ℓ = the integral length scale (outer scale) of the turbulent field

r = the characteristic dimension of the scattering volume.

The integral length scale is defined as

$$\ell = \frac{1}{\langle v(0)v(0)\rangle} \int_0^\infty \langle v(r)v(0)\rangle \, dr \qquad (22)$$

where

v = the turbulent fluctuation in the wind speed.

Hence, four parameters are needed to estimate probabilities of detection: C_T^2, C_V^2, ℓ, and r. We now discuss the physical meaning and methods for estimating each of the quantities.

4.1 Structure-Function Parameters

The behavior of the ensemble-mean structure-function parameters has been well studied and analyzed in recent years. The structure-function parameters can be calculated from

$$C_T^2 \cong 3\varepsilon_\theta \varepsilon^{-1/3} \qquad (23)$$

and

$$C_V^2 \cong 2\varepsilon^{2/3} \qquad (24)$$

where

ε = the dissipation rate of TKE

ε_θ = the destruction rate of temperature variance.

Estimation of the dissipation and destruction rates is easily accomplished if we understand some basic concepts of atmospheric turbulence production. The production comes from two types of instability: wind shear and buoyancy. Shear is most significant at high wind speeds. Shear production of TKE equals $u_*^3 / \kappa z$ where u_* is the friction velocity, $\kappa \approx 0.4$ is von Karman's constant, and z is the height. The friction velocity can be estimated from the wind velocity gradient:

$$u_* \cong \kappa z \frac{dU}{dz}. \qquad (25)$$

Buoyancy becomes a significant source of turbulence when there is solar heating of the ground, which makes the air near the ground warmer and less

dense than the overlying air. Buoyant production equals w_*^3 / z_i, where $w_* = (gQ_s z_i / T_s)^{1/3}$ is the convective velocity scale, g is gravitational acceleration, Q_s is the surface heat flux, z_i is the height of the boundary-layer capping inversion, and T_s is the surface temperature (Stull 1988).

The relative significance of shear and buoyant production depends on the height. In fact, if we take the ratio of buoyant to shear production, we have

$$\frac{u_*^3 / \kappa z}{w_*^3 / z_i} = \frac{z}{-L} \tag{26}$$

where the quantity $L = u_*^3 T_s / \kappa g Q_s$ is called the Obukhov length. Buoyancy production dominates when $z >> -L$. Shear production dominates when $z << -L$.

In the case where shear production dominates, by assuming that local production balances local dissipation (usually a good assumption), the TKE dissipation rate is simply

$$\varepsilon = u_*^3 / \kappa z . \tag{27}$$

When shear production dominates, parameterization of ε_ρ is unimportant because temperature fluctuations play an insignificant role in acoustic wave scattering.

Suppose conditions are freely convective (solar heating, as opposed to wind shear, is the primary source of the turbulence). The dissipation rate is

$$\varepsilon = w_*^3 / z_i . \tag{28}$$

Under freely convective conditions, the destruction rate of temperature is given by (Stull 1988, Eq. 9.6.4r)

$$\varepsilon_\theta = 0.43 \frac{w_* \theta_*^2}{z_i} \left(\frac{z}{z_i} \right)^{-4/3} \tag{29}$$

where $\theta_* = Q_s / w_*$ is the convective temperature scale.

Estimation and measurement of atmospheric boundary layer parameters such as z_i, Q_s, u_*, and w_* is one of the fundamental problems of micrometeorology. Refer to (Stull 1988) for a discussion of relevant issues. When measurements of these parameters are unavailable, Q_s and u_* can be determined reliably

using a surface-energy balance model (e.g., Rachele, Tunick, and Hansen 1995). The inversion height can be calculated using a boundary-layer evolution model such as Blackadar's (1978).

4.2 Integral Length Scale

Estimation of integral length scales is quite challenging, because of the anisotropy and inhomogeneity characteristic of atmospheric turbulence. A further complication arises when the velocity and temperature fields have their own length scales.

One of the most comprehensive, experimental studies of integral length scales in the atmospheric convective boundary layer was done by Lenschow and Stankov (1986). Using data from aircraft, Lenschow and Stankov found for the horizontal velocity fluctuations

$$\ell = 0.30 z_i \quad . \tag{30}$$

Equation (30) should work reasonably well in most situations of interest because it is, primarily, horizontal velocity fluctuations that drive the acoustic index of refraction during the daytime (Wilson and Thomson 1995).

Wilson and Thomson (1995) have proposed a more complicated model for integral length scales incorporating anisotropy, height-dependence, and the combined effects of velocity and temperature on the index of refraction. The model makes use of the same scaling parameters discussed in connection with structure-function parameter estimations. Although the equations are not given here, some example predictions are provided in figure 10. For these predictions, the friction velocity was set to 0.3 m/s, characteristic of moderate winds. The inversion height was 1000 m, a value representative of sunny days at most locations in temperate climates. Near the ground, the length scale is observed to be relatively independent of height. There is a strong dependence on surface heat flux. At greater heights ($z > 100$ m), the length scale is approximately independent of heat flux and has only a weak height dependence. At these heights, the Wilson and Thomson model is in reasonable agreement with equation (30).

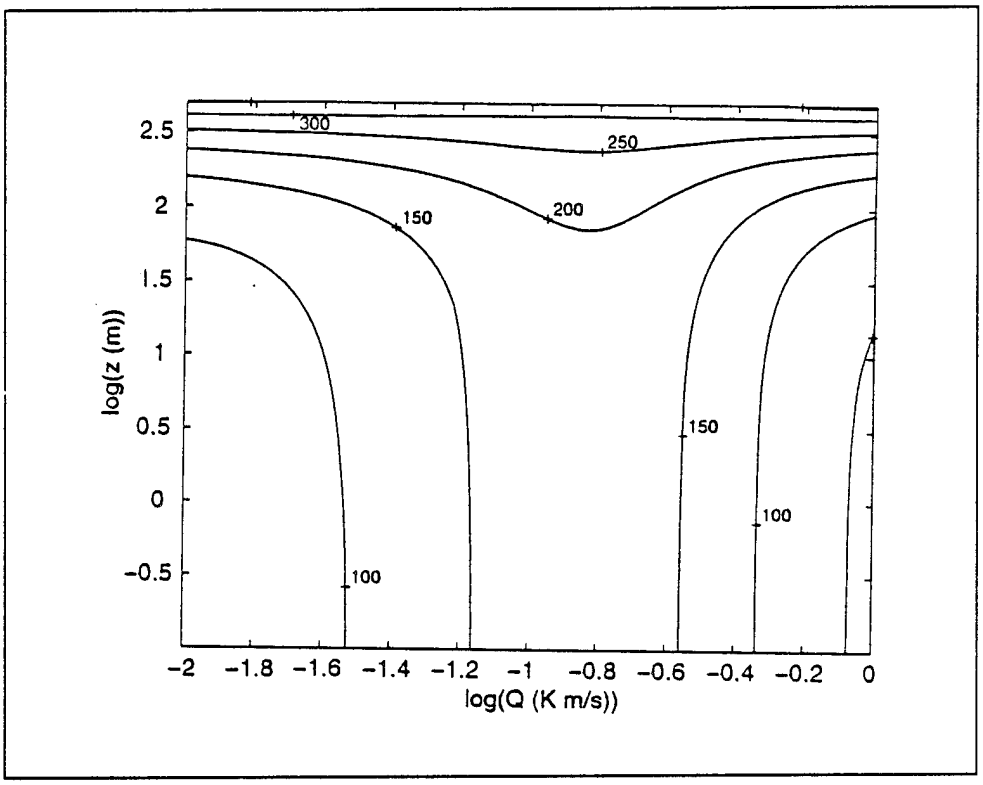

Figure 10. Integral length scale (m) as a function of height and surface heat flux, using the model of Wilson and Thomson (1994).

Broadly speaking, we expect ℓ to range from 10 to 1000 m, depending on the meteorological conditions. Smaller values are characteristic of near ground, high wind shear conditions, whereas larger values occur in highly convective, deep boundary layers.

4.3 Scattering Volume Dimensions

The characteristic length scale of the scattering volume depends on the beam patterns of the source and receiver, the local topography, and meteorological conditions. Presumably, if the spatial dimensions $(\Delta x, \Delta y, \Delta z)$ of the scattering volume are known, the single characteristic dimension needed by equation (21) could be determined from

$$r = (\Delta x \, \Delta y \, \Delta z)^{1/3} . \qquad (31)$$

There is little information on scattering volume dimensions for acoustic configurations of practical interest. Researchers only recently have begun to realize the significant role played by this parameter in scattering problems.

Among the few resources available on this topic are recent papers by Stinson, Havelock, and Daigle (1994) and Auvermann (1995).

Auvermann considered propagation over a 320-m path at a 500-Hz frequency. Scattering was modeled using the turbule ensemble model. Refraction effects were not explicitly considered in the calculation. Auvermann defined the scattering volume as the region from which 99.8 percent of the received signal originates. The dimensions of the scattering volume were found to decrease substantially as the size of the scattering eddies increased. Auvermann's calculations are summarized in table 1.

Table 1. Characteristic length *r* of the scattering volume, as a function of eddy size, at a 500-Hz frequency (Auvermann 1995)

Eddy size (m)	Characteristic length (m)
0.438	13.218
0.876	8.171
1.752	5.148
3.504	3.262
7.008	2.071
10.07	1.633

Stinson, Havelock, and Daigle (1994) used a Green's function parabolic equation (GF-PE) code to simulate the creation of a refractive shadow zone in the atmosphere. Random, Gaussian perturbations to the index-of-refraction field, having a 4-m characteristic length, were introduced to model turbulent scattering. Like Auvermann, Stinson used a 500-Hz frequency, but the 896-m propagation path was longer than Auvermann's. The extent of the scattering volume was depicted only graphically by Stinson, Havelock, and Daigle (1994); no explicit calculations of dimensions similar to Auvermann's were made. Stinson, Havelock, and Daigle's figure 9 suggests that their characteristic length r for the scattering is between 30 and 60 m. From table 1, it appears that Auvermann's model yields $r \approx 3$ m for the 4-m eddy size. The reason for this discrepancy is not entirely clear. Possible explanations are the neglect of refraction in Auvermann's model, the difference in the lengths of the propagation paths, or our nonrigorous estimate of the scattering volumes derived from the figure in Stinson, Havelock, and Daigle (1994).

Lacking further information, we should expect the characteristic dimension of the scattering volume to vary from about 1 to 100 m in most problems of interest. The primary determinants of this parameter should be the source/receiver configuration, acoustic frequency, and mean refractive profiles. With r in this range and ℓ in the range given at the end of the previous subsection, we have from equation (21)

$$0 < \sigma_\varepsilon^2 < 2 . \qquad (32)$$

More field measurements are needed to verify the range of values for the intermittency variance parameter.

5. Summary

The significant impact of turbulent intermittency on acoustic scattering statistics was demonstrated using experimental data and theoretical models. The main effect of intermittency is to increase the probability of occurrence of large values of the scattered intensity, which can be quite important in detection problems. In particular, the intermittency effect is important in environments with a fairly constant noise background.

Although theoretical models for the intermittency effect are reasonably simple, the parameters required by these models are still rather difficult to estimate. Our knowledge of turbulent length scales in the atmosphere is limited; we have even more difficulty providing representative values for the dimensions of acoustic scattering volumes. There is no reason why future research should not make substantial progress in addressing the issues.

References

Anselmet, F., Y. Gagne, E. Hopfinger, and R. A.. Antonia, "Higher-order Velocity Structure Functions in Turbulent Shear Flows," *J. Fluid Mech.*, **140**, p 63-89, 1984.

Auvermann, H. J., "Calculation of Scattering Volume Limits for Acoustical Scattering from Homogeneous Turbulence Using the Turbule Ensemble Model," In *Proceedings of the Sixth Annual Ground Target Modeling and Validation Conference,* Michigan Technological University, Houghton, 1995.

Blackadar, A. K., "Modeling Pollutant Transfer during Daytime Convection," In *Proceedings of the Fourth Symposium on Atmospheric Turbulence, Diffusion, and Air Quality* (Amer. Met. Soc, Reno), p 443–447, 1978.

Gilbert, K. E., R. Raspet, and X. Di, "Calculation of Turbulence Effects in an Upward-refracting Atmosphere," *J. Acoust. Soc. Am.*, **87**, p 2428–2437, 1990.

Gurvich, A. S., and Y. M. Yaglom, "Breakdown of Eddies and Probability Distributions for Small-scale Turbulence," *Phys. Fluids, Supplement on Boundary Layers and Turbulence*, S59–S65, 1967.

Kolmogorov, A. N., "A Refinement of Previous Hypotheses Concerning the Local Structure of Turbulence in a Viscous Incompressible Fluid at High Reynolds Number," *J. Fluid Mech.*, **13**, p 82–85, 1962.

Lenschow, D. H., and B. B. Stankov, "Length Scales in the Convective Boundary Layer," *J. Atmos. Sci.*, **43**, p 1198–1209, 1986.

Nakagami, M., "The m-distribution — A General Formula of the Intensity Distribution of Rapid Fading," *Statistical Methods in Radio Wave Propagation*, W. C. Hoffman, ed., Pergamon Press, Oxford, p 3–36, 1960.

Obukhov, A. M., "Some Specific Features of Atmospheric Turbulence," *J. Fluid Mech.*, **13**, p 77–81, 1962.

Ostashev, V. E., "Sound Propagation and Scattering in Media with Random Inhomogeneities of Sound Speed, Density and Medium Velocity," *Waves Rand. Med.*, **4**, p 403–428, 1994.

Rachele, H., A. Tunick, and F. V. Hansen, "MARIAH – A Similarity-based Method for Determining Wind, Temperature, and Humidity Profile Structure in the Atmospheric Surface Layer," *J. Appl. Meteor.*, **34**, p 1000–1005, 1995.

Rice, S. O., "Mathematical Analysis of Random Noise," *Bell System Tech. J.*, **24**, p 45–156, 1945.

Romano, G. P., "Scaling Exponents of Structure Functions in Near-wall Flows at Low Reynolds Numbers," In *Proceedings of the Tenth Symposium on Turbulent Shear Flows*, University Park, PA, p 17-25–17-30, 1995.

Stinson, M. R., D. I. Havelock, and G. A. Daigle, "Simulation of Scattering by Turbulence into a Shadow Region using the GF-PE Method," In *Proceedings of the Sixth International Symposium on Long-Range Sound Propagation*, Ottawa, p 283–295, 1994.

Stull, R. B., *An Introduction to Boundary Layer Meteorology*, Kluwer, Dordrecht, 1988.

Tatarskii, V. I., *The Effects of the Turbulent Atmosphere on Wave Propagation*, Keter, Jerusalem, 1971.

Wilson, D. K., "Scattering of Acoustic Waves by Intermittent Temperature and Velocity Fluctuations," submitted to *J. Acoust. Soc. Am.*, 1995.

Wilson, D. K., and D. W. Thomson, "Acoustic Propagation through Anisotropic, Surface-layer Turbulence," *J. Acoust. Soc. Am.*, **96**, p 1080–1095, 1995.

Wilson, D. K., J. C. Wyngaard, and D. I. Havelock, "The Effect of Turbulent Intermittency on Scattering into an Acoustic Shadow Zone," *J. Acoust. Soc. Am.*, 1995.

Acronyms and Abbreviations

pdf	probability distribution function
SNR	signal-to-noise ratio
TKE	turbulent kinetic energy

Distribution

	Copies
NASA MARSHAL SPACE FLT CTR ATMOSPHERIC SCIENCES DIV E501 ATTN DR FICHTL HUNTSVILLE AL 35802	1
NASA SPACE FLT CTR ATMOSPHERIC SCIENCES DIV CODE ED 41 1 HUNTSVILLE AL 35812	1
ARMY STRAT DEFNS CMND CSSD SL L ATTN DR LILLY PO BOX 1500 HUNTSVILLE AL 35807-3801	1
ARMY MISSILE CMND AMSMI RD AC AD ATTN DR PETERSON REDSTONE ARSENAL AL 35898-5242	1
ARMY MISSILE CMND AMSMI RD AS SS ATTN MR H F ANDERSON REDSTONE ARSENAL AL 35898-5253	1
ARMY MISSILE CMND AMSMI RD AS SS ATTN MR B WILLIAMS REDSTONE ARSENAL AL 35898-5253	1
ARMY MISSILE CMND AMSMI RD DE SE ATTN MR GORDON LILL JR REDSTONE ARSENAL AL 35898-5245	1
ARMY MISSILE CMND REDSTONE SCI INFO CTR AMSMI RD CS R DOC REDSTONE ARSENAL AL 35898-5241	1

ARMY MISSILE CMND
AMSMI
REDSTONE ARSENAL
AL 35898-5253 1

CMD 420000D C0245
ATTN DR A SHLANTA
NAVAIRWARCENWPNDIV
1 ADMIN CIR
CHINA LAKE CA 93555-6001 1

PACIFIC MISSILE TEST CTR
GEOPHYSICS DIV
ATTN CODE 3250
POINT MUGU CA 93042-5000 1

LOCKHEED MIS & SPACE CO
ATTN KENNETH R HARDY
ORG 91 01 B 255
3251 HANOVER STREET
PALO ALTO CA 94304-1191 1

NAVAL OCEAN SYST CTR
CODE 54
ATTN DR RICHTER
SAN DIEGO CA 92152-5000 1

METEOROLOGIST IN CHARGE
KWAJALEIN MISSILE RANGE
PO BOX 67
APO SAN FRANCISCO
CA 96555 1

DEPT OF COMMERCE CTR
MOUNTAIN ADMINISTRATION
SPPRT CTR LIBRARY R 51
325 S BROADWAY
BOULDER CO 80303 1

DR HANS J LIEBE
NTIA ITS S 3
325 S BROADWAY
BOULDER CO 80303 1

NCAR LIBRARY SERIALS
NATL CTR FOR ATMOS RSCH
PO BOX 3000
BOULDER CO 80307-3000 1

DEPT OF COMMERCE CTR
325 S BROADWAY
BOULDER CO 80303 1

DAMI POI
WASH DC 20310-1067 1

MIL ASST FOR ENV SCI OFC
OF THE UNDERSEC OF DEFNS
FOR RSCH & ENGR R&AT E LS
PENTAGON ROOM 3D129
WASH DC 20301-3080 1

DEAN RMD
ATTN DR GOMEZ
WASH DC 20314 1

ARMY INFANTRY
ATSH CD CS OR
ATTN DR E DUTOIT
FT BENNING GA 30905-5090 1

AIR WEATHER SERVICE
TECH LIBRARY FL4414 3
SCOTT AFB IL 62225-5458 1

USAFETAC DNE
ATTN MR GLAUBER
SCOTT AFB IL 62225-5008 1

HQ AWS DOO 1
SCOTT AFB IL 62225-5008 1

PHILLIPS LABORATORY
PL LYP
ATTN MR CHISHOLM
HANSCOM AFB MA 01731-5000 1

ATMOSPHERIC SCI DIV
GEOPHYSICS DIRCTRT
PHILLIPS LABORATORY
HANSCOM AFB MA 01731-5000 1

PHILLIPS LABORATORY
PL LYP 3
HANSCOM AFB MA 01731-5000 1

RAYTHEON COMPANY
ATTN DR SONNENSCHEIN
528 BOSTON POST ROAD
SUDBURY MA 01776
MAIL STOP 1K9 1

ARMY MATERIEL SYST 1
ANALYSIS ACTIVITY
AMXSY
ATTN MP H COHEN
APG MD 21005-5071

ARMY MATERIEL SYST 1
ANALYSIS ACTIVITY
AMXSY AT
ATTN MR CAMPBELL
APG MD 21005-5071

ARMY MATERIEL SYST 1
ANALYSIS ACTIVITY
AMXSY CR
ATTN MR MARCHET
APG MD 21005-5071

ARL CHEMICAL BIOLOGY 1
NUC EFFECTS DIV
AMSRL SL CO
APG MD 21010-5423

ARMY MATERIEL SYST 1
ANALYSIS ACTIVITY
AMXSY
APG MD 21005-5071

ARMY MATERIEL SYST 1
ANALYSIS ACTIVITY
AMXSY CS
ATTN MR BRADLEY
APG MD 21005-5071

ARMY RESEARCH LABORATORY 1
AMSRL D
2800 POWDER MILL ROAD
ADELPHI MD 20783-1145

ARMY RESEARCH LABORATORY 1
AMSRL OP SD TP
TECHNICAL PUBLISHING
2800 POWDER MILL ROAD
ADELPHI MD 20783-1145

ARMY RESEARCH LABORATORY 1
AMSRL OP CI SD TL
2800 POWDER MILL ROAD
ADELPHI MD 20783-1145

ARMY RESEARCH LABORATORY 1
AMSRL SS SH
ATTN DR SZTANKAY
2800 POWDER MILL ROAD
ADELPHI MD 20783-1145

ARMY RESEARCH LABORATORY 1
AMSRL
2800 POWDER MILL ROAD
ADELPHI MD 20783-1145

NATIONAL SECURITY AGCY W21 1
ATTN DR LONGBOTHUM
9800 SAVAGE ROAD
FT GEORGE G MEADE
MD 20755-6000

OIC NAVSWC 1
TECH LIBRARY CODE E 232
SILVER SPRINGS
MD 20903-5000

ARMY RSRC OFC 1
AMXRO GS
ATTN DR BACH
PO BOX 12211
RTP NC 27709

DR JERRY DAVIS 1
NCSU
PO BOX 8208
RALEIGH NC 27650-8208

US ARMY CECRL 1
CECRL GP
ATTN DR DETSCH
HANOVER NH 03755-1290

ARMY ARDEC 1
SMCAR IMI I BLDG 59
DOVER NJ 07806-5000

ARMY SATELLITE COMM AGCY 1
DRCPM SC 3
FT MONMOUTH NJ 07703-5303

ARMY COMMUNICATIONS 1
ELECTR CTR FOR EW RSTA
AMSEL EW D
FT MONMOUTH NJ 07703-5303

ARMY COMMUNICATIONS
ELECTR CTR FOR EW RSTA
AMSEL EW MD
FT MONMOUTH NJ 07703-5303 1

ARMY DUGWAY PROVING GRD
STEDP MT DA L 3
DUGWAY UT 84022-5000 1

ARMY DUGWAY PROVING GRD
STEDP MT M
ATTN MR BOWERS
DUGWAY UT 84022-5000 1

DEPT OF THE AIR FORCE
OL A 2D WEATHER SQUAD MAC
HOLLOMAN AFB
NM 88330-5000 1

PL WE
KIRTLAND AFB NM
87118-6008 1

USAF ROME LAB TECH
CORRIDOR W STE 262 RL SUL
26 ELECTR PKWY BLD 106
GRIFFISS AFB
NY 13441-4514 1

AFMC DOW
WRIGHT PATTERSON AFB
OH 0334-5000 1

ARMY FIELD ARTLLRY SCHOOL
ATSF TSM TA
FT SILL OK 73503-5600 1

NAVAL AIR DEV CTR
CODE 5012
ATTN AL SALIK
WARMINISTER PA 18974 1

ARMY FOREGN SCI TECH CTR
CM
220 7TH STREET NE
CHARLOTTESVILLE
VA 22901-5396 1

NAVAL SURFACE WEAPONS CTR
CODE G63
DAHLGREN VA 22448-5000 1

ARMY OEC
CSTE EFS
PARK CENTER IV
4501 FORD AVE
ALEXANDRIA VA 22302-1458 1

ARMY CORPS OF ENGRS
ENGR TOPOGRAPHICS LAB
ETL GS LB
FT BELVOIR VA 22060 1

ARMY TOPO ENGR CTR
CETEC ZC 1
FT BELVOIR VA 22060-5546 1

LOGISTICS CTR
ATCL CE
FT LEE VA 23801-6000 1

SCI AND TECHNOLOGY
101 RESEARCH DRIVE
HAMPTON VA 23666-1340 1

ARMY NUCLEAR CML AGCY
MONA ZB BLDG 2073
SPRINGFIELD VA 22150-3198 1

USATRADOC
ATCD FA
FT MONROE VA 23651-5170 1

ARMY TRADOC ANALYSIS CTR
ATRC WSS R
WSMR NM 88002-5502 1

ARMY RESEARCH LABORATORY
AMSRL BE S
BATTLEFIELD ENVIR DIR
WSMR NM 88002-5501 1

ARMY RESEARCH LABORATORY
AMSRL BE W
BATTLEFIELD ENVIR DIR
WSMR NM 88002-5501 1

ARMY RESEARCH LABORATORY
AMSRL BE
ATTN MR VEAZY
BATTLEFIELD ENVIR DIR
WSMR NM 88002-5501 1

DTIC 8725 JOHN J KINGMAN RD SUITE 0944 FT BELVOIR VA 22060-6218	1
ARMY MISSILE CMND AMSMI REDSTONE ARSENAL AL 35898-5243	1
ARMY DUGWAY PROVING GRD STEDP 3 DUGWAY UT 84022-5000	1
USATRADOC ATCD FA FT MONROE VA 23651-5170	1
WSMR TECH LIBRARY BR STEWS IM IT WSMR NM 88001	1
Record Copy	2
TOTAL	77